

## SHORT REPORT

A locus for asphyxiating thoracic dystrophy, *ATD*, maps to chromosome 15q13

N V Morgan, C Bacchelli, P Gissen, J Morton, G B Ferrero, M Silengo, P Labrune, I Casteels, C Hall, P Cox, D A Kelly, R C Trembath, P J Scambler, E R Maher, F R Goodman, C A Johnson

*J Med Genet* 2003;40:431–435

Asphyxiating thoracic dystrophy (ATD), or Jeune syndrome, is a multisystem autosomal recessive disorder associated with a characteristic skeletal dysplasia and variable renal, hepatic, pancreatic, and retinal abnormalities. We have performed a genome wide linkage search using autozygosity mapping in a cohort of four consanguineous families with ATD, three of which originate from Pakistan, and one from southern Italy. In these families, as well as in a fifth consanguineous family from France, we localised a novel ATD locus (*ATD*) to chromosome 15q13, with a maximum cumulative two point lod score at D15S1031 ( $Z_{\max}=3.77$  at  $\theta=0.00$ ). Five consanguineous families shared a 1.2 cM region of homozygosity between D15S165 and D15S1010. Investigation of a further four European kindreds, with no known parental consanguinity, showed evidence of marker homozygosity across a similar interval. Families with both mild and severe forms of ATD mapped to 15q13, but mutation analysis of two candidate genes, *GREMLIN* and *FORMIN*, did not show pathogenic mutations.

Asphyxiating thoracic dystrophy (ATD, MIM 208500), also known as Jeune syndrome, is an autosomal recessive multisystem developmental disorder,<sup>1</sup> characterised by abnormal skeletal development, with typical radiographical findings (fig 1) that include a long, narrow, "bell shaped" thorax with short, abnormal ribs, metaphyseal irregularities, and short long bones (involving predominately the ulnae, radii, fibulae, and tibiae).<sup>2,4</sup> Clavicles can be abnormal ("bicycle handlebar shaped") and cone shaped epiphyses of the hands and abnormalities of the pelvis are considered to be diagnostic.<sup>2</sup> Features of the latter, in the neonatal period, comprise small ilia and irregularity of the acetabulum ("trident shaped"), from which a medial and lateral bony projection is visible. Renal, hepatic, pancreatic, and retinal abnormalities are common features of ATD and polydactyly of both hands and/or feet has been reported.

ATD shows wide phenotypic variability and cases have been classified into lethal, severe, mild, and latent forms.<sup>5</sup> Most patients are severely affected and die from asphyxia caused by a small thorax and hypoplastic lungs, in the perinatal period. However, approximately one-fifth of children with ATD survive beyond the neonatal period, only to develop significant renal impairment, with cystic changes and periglomerular fibrosis leading to chronic renal failure.<sup>6</sup> Liver involvement may be severe and biliary cirrhosis can cause early morbidity.<sup>7,8</sup> While ophthalmological involvement is not a presenting symptom, retinal dystrophy is an occasional feature.<sup>9</sup> The molecular basis of ATD is at present unknown, with few clues to the location of genes likely to contribute to pathogenesis. A similar phenotype occurs in Ellis-van Creveld

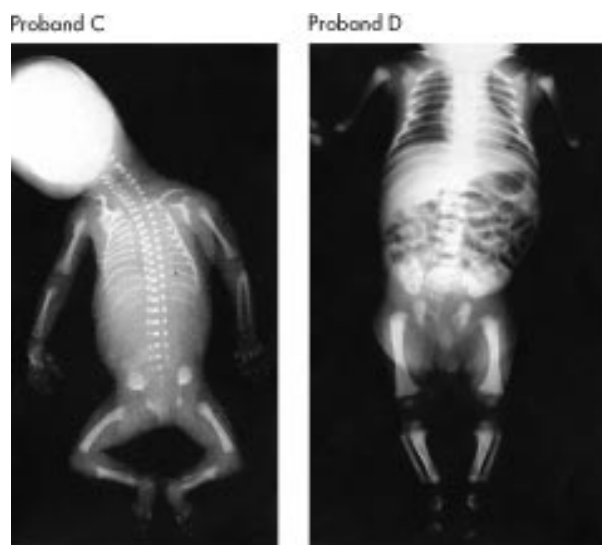


**Figure 1** Radiographs of probands C (left) and D (right), showing the typical skeletal abnormalities of ATD. C was stillborn at 30/40, and the radiograph of D is at 3 months of age. Both probands have short horizontal ribs, narrow, "bell shaped" thoraces, mesomelic shortening in the lower limbs, and abnormalities of the pelvis. Medial and lateral bony projections are present on the acetabular roof of C.

syndrome (EVC, MIM 225500), and has been reported in one case with a de novo deletion of chromosome 12p11-p12.<sup>10</sup> A mouse model of ATD has been proposed, known as the shorty (*srt*) mutant, identified through a screen of recessive developmental mutations.<sup>11</sup> The human chromosomal regions syntenic to the *srt* locus are chromosome 6p21, 6q25-27, and 16p13.3.

#### MATERIAL AND METHODS

To determine the molecular basis of ATD we ascertained five consanguineous families containing a single affected subject and performed autozygosity mapping studies (fig 2). Informed consent was obtained from these families and the study was approved by the relevant Local Research Ethics Committees. Clinical notes and pedigrees indicated that the parents in families A to D are first cousins. In family E, there is anecdotal evidence of consanguinity (P Lebrune, personal communication), and the parents are thought to be first cousins. Three families originated from Pakistan (A-C) and are resident in the UK. Although families A-C originate from a relatively isolated region of Pakistan, Mirpur, the families are not known to be related. Family D and E originate from southern Italy and France, respectively. Clinical assessment supports a diagnosis in the probands as either severe (families

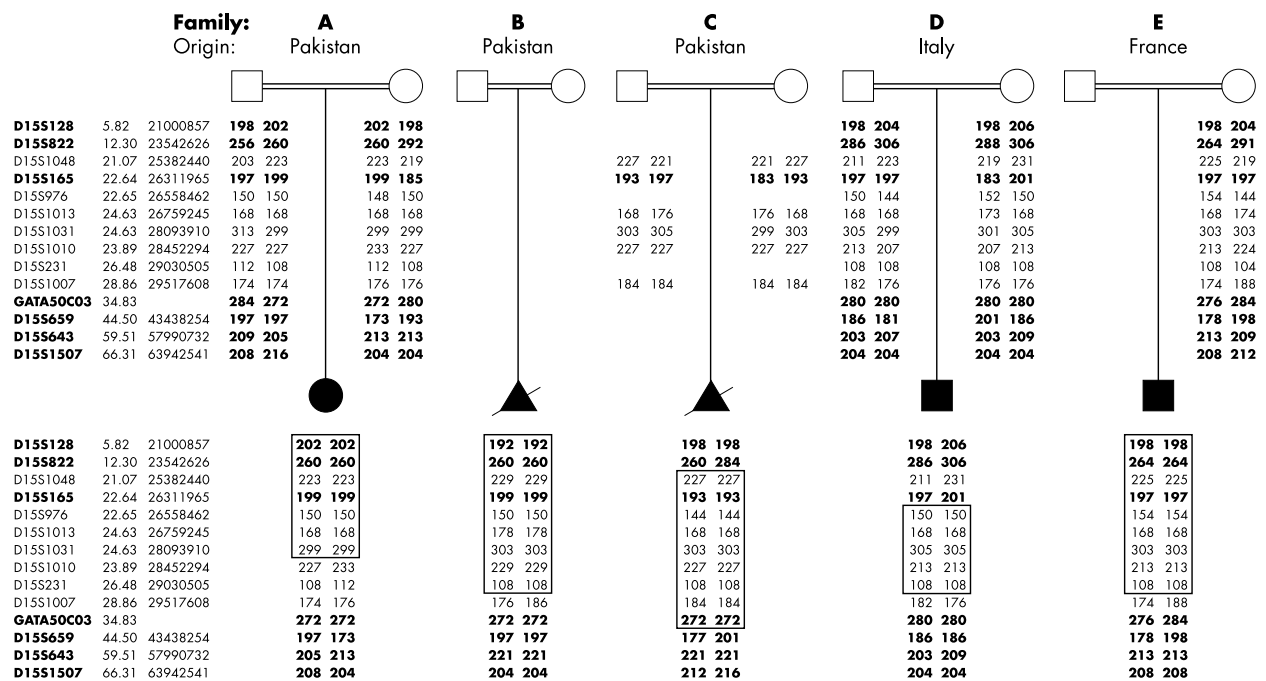


**Figure 2** Haplotypes for 14 markers from chromosome 15q13 in four consanguineous families A to E with ATD. The origin of each family is indicated at the top, and affected probands are shown by filled symbols. The genetic distance of each marker is taken from the high resolution deCODE genetic map and listed on the left. The physical position of the forward strand start of the microsatellite sequence is also listed. Markers included in the original genome wide linkage search are shown in bold. Boxes around marker alleles indicate the regions of homozygosity. The minimal candidate interval that encompasses the ATD locus is the region between D15S165 and D15S1010.

B and C) or mild (families A, D and E) ATD. In all cases the diagnosis of ATD was confirmed by a perinatal pathologist and/or a radiologist specialising in skeletal malformation syndromes and a neonatal skeletal survey showed typical features of ATD (short horizontal ribs, with small narrow thoraces; acetabular roofs were horizontal, with medial and lateral spurs) in all cases (fig 1). In the case of proband B, a therapeutic termination of pregnancy was performed following an ultrasound diagnosis of ATD during the second trimester.<sup>12</sup> Affected fetus C was stillborn at 30 weeks. Probands A and D were aged 36 and 30 months, respectively, at the time of the study, and have normal renal function and no evidence of liver disease. Full details of proband E have been published elsewhere (case 3 in Lebrune *et al*<sup>8</sup>). He developed biliary cirrhosis at 25 months, but subsequent cholestasis was controlled by treatment with ursodeoxycholic acid, with biliary acid and serum concentrations in the normal range, and no evidence of impaired renal function at age 11 years. The relevant clinical and radiographic findings for probands A to E are summarised in table 1.

In the first instance we investigated whether ATD was linked to previously suggested candidate regions (the *EVC* gene, 12p11-p12, and 6p21, 6q25-27, and 16p13.3 that are syntenic to the 7 cM interval on mouse chromosome 17 to which *srt* has been mapped). Analysis of haplotypes in families A-D excluded linkage to all of these regions (data not shown). To map a locus for ATD, we performed a genome wide linkage search in the four affected subjects, using an autozygosity mapping approach. Four hundred microsatellite markers, spaced at 10 cM intervals, from the Research Genetics linkage mapping set version 10, were amplified by PCR as described previously.<sup>13</sup> PCR products were electrophoresed on an ABI 377 DNA Analyzer, and were analysed with Genescan v3.1.2 and Genotyper v2.5.2 software (Applied Biosystems). ATD was modelled as a fully penetrant autosomal recessive condition, with a disease allele frequency of 0.001. Alleles for marker loci were assumed to be codominant and to occur at equal frequencies, because population allele frequencies were

not available. Two point lod scores were calculated with the MLINK program in the LINKAGE (version 5.1) software package.<sup>14</sup> In addition to the proband and parents, the input files that defined the pedigree structure also included additional family members to create a first cousin consanguineous "loop".<sup>14</sup>

## RESULTS

The data from the original genome wide linkage search showed extended regions of homozygosity in probands A (29 cM from D15S128 to GATA50C03) and B (54 cM, D15S128 to D15S1507) (fig 2, markers shown in bold). No other regions of homozygosity, that were common to the four probands A to D, were found in the genome wide linkage search. These subjects were homozygous for the same allele at D15S822 and D15S165, and all Pakistani probands (A to C) were homozygous for the same allele at GATA50C03. The Italian proband, D, was homozygous at GATA50C03 and D15S659. This suggested that the gene for ATD was located between D15S822 and D15S659, an interval of 31 cM, on chromosome 15q13. To fine map this interval, we genotyped an additional seven microsatellite markers in all four affected probands (A to D) and their parents, as well as proband E and his mother (fig 2, markers shown in plain text). DNA was not available from the parents of proband B or the father of proband E. Suitable markers were identified from the Marshfield mapping panels<sup>15</sup> (Marshfield Medical Research Foundation; [http://research.marshfieldclinic.org/genetics/Map\\_Markers/](http://research.marshfieldclinic.org/genetics/Map_Markers/)) and their physical and genetic locations determined from both the Ensembl Genome Browser database ([http://www.ensembl.org/Homo\\_sapiens/](http://www.ensembl.org/Homo_sapiens/)) and the deCODE Genetics high resolution genetic map.<sup>16</sup> The order and distance between these markers was based on the deCODE map. The five probands were homozygous for markers D15S976, D15S1013, and D15S1031. The Pakistani probands A and C were homozygous for the same alleles at marker D15S1013, whereas B and C were identical at D15S1031 (fig 2). A common 1.2 cM region of homozygosity between markers

**Table 1** Radiographic and clinical features of probands A to H

	Proband							
	A	B	C	D	E	F	G	H
Country of origin	Pakistan	Pakistan	Pakistan	Italy	France	Italy	Italy	Belgium
Degree of parental consanguinity	First cousins Female	First cousins Male	First cousins Male	First cousins Male	First cousins Male	Distant? Male	None known Female	None known Female
Sex	Female	Male	Male	Male	Male	Male	Female	Female
Age (months)	39	Termination 21+/40	Miscarriage 20/40	33	132	55	41	118
Length at birth (cm)	44 (at 34/40)	29	24	40	Not known	49	46	51
Birth weight (g)	1965 (at 34/40)	643	242	2490	3310	3560	3150	3200
Short horizontal ribs & narrow thorax	+	+	+	+	+	+	+	+
Short limbs (upper/lower)	+/+	-/- mild bowing of humeri & femora	-/+	+/+	+/+	-/+ shortening of femora	+/+	+/+
Trident acetabulum, (with medial/lateral spurs)	+	+	+	+	+	+	+	+
Bilateral postaxial polydactyly (hands/feet)	Not known	-/-	-/-	-/-	-/-	-/-	+/+	+/+
Respiratory problems in neonatal period	+	N/A	N/A	-	+	+	-	-
Liver function	Normal	Abnormal ductal plates in liver	No abnormalities detected	Normal	Neonatal conjugated hyperbilirubinaemia; biliary cirrhosis at 25 months	Normal	Normal	Normal
Renal function	Normal	Mild dilatation of some tubules	No abnormalities detected	Normal	Normal	Normal	Normal	Normal
Ophthalmological findings	Rod/cone dystrophy at 9 months	N/A	N/A	Normal	Normal	Normal	Normal	Retinal dystrophy at 66 months
Other findings	Handlebar shaped clavicles	Hypoplastic middle phalanges of hands	Short middle phalanges	Chest circumference below 3rd centile				Cone shaped epiphyses of phalanges

+ denotes presence and - denotes absence of a feature; N/A not applicable.

**Table 2** Maximum cumulative two point lod scores for the ATD locus and markers from chromosome 15q13 in consanguineous families A to E

Marker	Lod score at $\theta=$				
	0.000	0.050	0.100	0.200	0.300
D15S1048	1.561	2.659	2.420	1.696	0.985
D15S165	0.938	2.130	1.939	1.326	0.744
D15S976	0.433	1.744	1.556	0.993	0.507
D15S1013	2.963	2.468	1.997	1.175	0.568
D15S1031	3.774	3.225	2.690	1.705	0.916
D15S1010	2.819	2.088	1.870	1.211	0.604
D15S231	-0.464	1.203	1.091	0.682	0.337

D15S165 and D15S1010 was detected in all five probands. A maximum cumulative two point lod score was detected at D15S1031 ( $Z_{max}=3.77$  at  $\theta=0.00$ ) (table 2).

**DISCUSSION**

In certain recessive disorders, the identification of the disease gene has been expedited by the detection of allelic homozygosity in apparently non-consanguineous families. Thus in the search for *NPHP4*, homozygosity within the critical interval was detected in affected subjects from a family initially thought to be non-consanguineous, but in which distant consanguinity was eventually shown.<sup>17</sup> To determine whether such an approach might be useful in sublocalising the *ATD* gene on chromosome 15q13, we ascertained three additional non-consanguineous European families with ATD (families F to H, fig 2). Families F and G originated from southern Italy. There is anecdotal evidence of distant consanguinity in family F, and both grandmothers of the proband originate from the same village in southern Italy (M Silengo, personal communication). Proband F had severe respiratory distress at birth, which eventually required tracheostomy, because of an extremely hypoplastic, short thorax. At the age of 53 months there is no evidence of renal disease. Proband G was noted to have postaxial polydactyly of both hands and feet. Skeletal x rays for both probands F and G were diagnostic for ATD, showing shortening of the long bones and typical acetabular spurs (M Silengo, personal communication). Proband H also had a typical ATD phenotype<sup>18</sup> and the family originates from Belgium. The affected child appeared to have a mild form of ATD, with typical features that include bilateral postaxial polydactyly, but presented with retinal dystrophy at the age of 5½ years.<sup>18</sup> There was no evidence of renal or liver disease. Clinical and radiographic findings for probands F to H are summarised in table 1.

Families F to H were genotyped for the 14 microsatellite markers from the chromosome 15q interval that defined the haplotypes of families A to E (fig 3). Although the parents in families F to H are not known to be related, the haplotypes of the affected children contain small regions of homozygosity within the D15S165 to D15S1010 interval. The unaffected sib of proband F was heterozygous throughout this interval. Homozygosity in the affected children F to H may have arisen from distant consanguinity in these families. Probands D to H all share identical homozygous alleles at markers D15S1013 and D15S231 (fig 3), although the heterozygosity h of these markers is 0.53 and 0.50, respectively. Marker D15S976 ( $h=0.63$ ) shares alleles for probands D, F, G, and H, D15S1010 ( $h=0.80$ ) has identical homozygous alleles for D and E and different but homozygous alleles for G and H. These data support the previous conclusion that the *ATD* locus maps within a 1.2 cM interval from D15S165 to D15S1010, and may reduce the candidate interval to between D15S165 and D15S1031. Although homozygosity could also indicate that alleles for the

Marker	Family:	D	F	G	H	E
	Origin:	Italy	Italy	Italy	Belgium	France
D15S128		198 206	198 206	200 200	198 200	198 198
D15S822		286 306	286 282	286 286	290 290	264 264
D15S1048		211 231	201 201	229 229	219 219	225 225
D15S165		197 201	199 199	203 184	197 197	197 197
D15S976		150 150	150 150	150 150	150 150	154 154
D15S1013		168 168	168 168	168 168	168 168	168 168
D15S1031		305 305	303 303	299 299	301 299	303 303
D15S1010		213 213	233 229	227 227	227 227	213 213
D15S231		108 108	108 108	108 108	108 108	108 108
D15S1007		182 176	180 176	176 176	182 178	174 188
GATA50C03		280 280	276 276	280 280	272 284	276 284
D15S659		186 186	198 178	182 198	194 198	178 198
D15S643		203 209	205 209	203 199	205 221	213 213
D15S1507		204 204	204 208	208 204	204 204	208 208

**Figure 3** Haplotypes for the same 14 markers as shown in fig 2 in probands D, E, and three additional probands with ATD (F to H), who are children of non-consanguineous parents. The origin of each family is indicated at the top. Boxes around marker alleles indicate the regions of homozygosity, and grey shading indicates alleles that are both homozygous and identical to those in proband D. The approximate positions of the candidate genes, *GREMLIN* and *FORMIN*, are indicated (see text for details).

markers in this region are identical by state, the alleles at most of the markers in this interval for the European cohort (D to H) differ from those of the consanguineous Pakistani cohort (A to C).

Scrutiny of the Ensembl Genome Browser database and the "Golden Path" June 2002 Build 30 human genome assembly at the UCSC Genome Browser (<http://genome.cse.ucsc.edu/>) showed that the minimal critical interval of D15S165 to D15S1010 was 1.5 Mb in size and contains seven known genes and nine predicted genes. Two of the known genes, *GREMLIN* and *FORMIN*, appeared to be excellent candidates for ATD. *GREMLIN* maps to a position proximal but adjacent to D15S1010, and both D15S1010 and D15S231 are intragenic with respect to *FORMIN* (fig 3). *FORMIN* on the reverse strand is adjacent to *GREMLIN* on the forward strand. Gremlin protein, also known as CKTSF1B1 (cystine knot superfamily 1, bone morphogenetic protein (BMP) antagonist 1), is predicted to be a small, secreted protein of 184 amino acids that contains a highly conserved cysteine rich repeat region, termed a cystine knot. This structural protein motif is shared by a superfamily that includes members of the transforming growth factor (TGF) $\beta$  family, the Norrie disease protein, the mucins, and von Willebrand factor. A role in early development and tissue specific differentiation for gremlin is inferred from the highly conserved homologues in *Xenopus*<sup>19</sup> and rat.<sup>20</sup> *Xenopus* Gremlin was shown to act as an antagonist of BMP signalling in embryonic explants,<sup>19</sup> presumably by binding BMPs and hence preventing their interaction with receptors. The biochemical characterisation of rat Gremlin showed that it could bind to BMP-4 in vitro.<sup>20</sup> This mechanism is similar to that of the proteins encoded by the pattern-inducing genes *noggin* and *chordin*.<sup>21-22</sup> The novel gene *SOST* encodes sclerostin, another member of the cystine knot superfamily, and closely related to Gremlin. Mutations in *SOST* cause sclerosteosis (*SOST*, MIM 269500), a severe sclerosing skeletal dysplasia characterised by bone overgrowth and syndactyly.<sup>23</sup> *GREMLIN* therefore represented an excellent candidate gene, since it encodes a protein that is a regulator during early development of bones and terminally differentiated tissues.

BMP antagonism by Gremlin relays signalling by Sonic hedgehog (SHH) during outgrowth and patterning of the vertebrate limb.<sup>24</sup> Mesenchymal *Gremlin* expression is lost in the limb buds of mouse embryos homozygous for recessive limb deformity (*ld*) mutations, which disrupt the *Formin* gene.<sup>25-26</sup> The *ld* phenotype is characterised by synostoses and syndactyly of all four limbs, and a renal defect that consists of either unilateral or bilateral renal dysplasia. *Formin* is therefore thought to be a morphoregulatory gene that regulates

epithelial-mesenchyme interactions during the patterning of limb skeletal elements and the induction of metanephric kidneys, and the human *FORMIN* gene is therefore a second candidate gene for ATD. None of the haplotypes for any family preclude *FORMIN* as a candidate, since both D15S1010 and D15S231 are intragenic. Proband A, for example, has an extended region of homozygosity that spans the region proximal to D15S1010.

We initially analysed the *GREMLIN* gene by direct sequencing of the single coding exon and exon/intron boundaries in all probands from families A to H. The only sequence change found was a SNP in the 3'UTR of the gene, \*+40 C>A. Proband C and E were homozygous for the A allele, and G was heterozygous for the SNP. All of the remaining probands were homozygous for the C allele. The heterozygous SNP in proband G therefore reduces the region of homozygosity in this affected subject to between markers D15S165 and D15S1031 (fig 3). The *FORMIN* gene spans 380 kb of genomic DNA and contains 18 coding exons. We designed primers to PCR the coding region and splice site boundaries (primer sequences can be supplied on request). Direct sequencing of the PCR products in all probands did not show any pathogenic mutations, although numerous homozygous SNPs were found in both coding and intronic sequences. Putative missense mutations were excluded as pathogenic by one or more of the following three criteria: the presence of homozygotes in normal controls, absence of segregation with disease phenotype in ATD families and/or lack of conservation of the mutated amino acid in the Formin sequences from other eukaryotic species. Thus, although both *FORMIN* and *GREMLIN* appeared to represent excellent candidate genes, we could not detect evidence of a pathogenic mutation in either gene. However, a mutation in a regulatory region or deep within an intron cannot be excluded. Studies of additional ATD families will refine the localisation of the gene and provide a basis for further candidate gene analysis. Genotyping additional markers within the candidate interval will confirm if a common ancestral haplotype exists in the cohort of European patients, as suggested by the block of shared homozygosity in probands D, F, G, and H centred on markers D15S976 and D15S1013 (fig 3). It remains to be determined whether other families with similar or overlapping phenotypes also show linkage to the same region. Preliminary work on further ATD families (both consanguineous and non-consanguineous) suggest that not all of them are linked to chromosome 15, indicating that ATD is likely to be genetically heterogeneous.

The identification of the ATD gene(s) will enable the development of molecular diagnostic tests to facilitate genetic

counselling, carrier testing, and prenatal diagnosis. Interestingly, both severe and mild forms of ATD mapped to 15q13, suggesting that phenotypic variation in ATD reflects allelic heterogeneity and not locus heterogeneity. Identification of the ATD gene(s) may provide important molecular insights into fundamental developmental pathways.

## ACKNOWLEDGEMENTS

The authors thank the families for their participation in this study, which was supported by the Wellcome Trust (UK Autozygosity Mapping Consortium: ERM, RCT), an Endowment Fund from Birmingham Children's Hospital Liver Unit (PG, CAJ), and a start up grant from the Birth Defects Foundation (CAJ). PG is a RCPC and Children Nationwide clinical research fellow in paediatric hepatology. GBF and MS are supported by grants from Compagnia di San Paolo, Torino, and MURST (grant number 06182533). We are grateful to a number of clinical colleagues for help in contacting families, including Dr Louise Bructon and Dr Jill Clayton-Smith.

## Authors' affiliations

**N V Morgan, P Gissen, E R Maher, C A Johnson**, Section of Medical and Molecular Genetics, Department of Paediatrics and Child Health, University of Birmingham Medical School, Birmingham B15 2TT, UK  
**C Bacchelli, P J Scambler, F R Goodman**, Molecular Medicine Unit, Institute of Child Health, 30 Guilford Street, London, WC1N 1EH, UK  
**P Gissen, D A Kelly**, Children's Liver Unit, Princess of Wales Children's Hospital, Steelhouse Lane, Birmingham B4 6NH, UK  
**J Morton**, West Midlands Regional Clinical Genetics Service, Birmingham Women's Hospital, Birmingham, B15 2TG, UK  
**G B Ferrero, M Silengo**, Dipartimento di Scienze Pediatriche e dell'Adolescenza, Università degli Studi di Torino, Piazza Polonia 94, 10126 Torino, Italy  
**P Labrunne**, Service de Pédiatrie, Hôpital Antoine-Béclère, 157 Rue de la Porte-de-Trivaux BP 405, 92141 Clamart, France  
**I Casteels**, Department of Paediatric Ophthalmology, St Rafael University Hospital, Capucijnenvoer 33, 3000 Leuven, Belgium  
**C Hall**, Department of Radiology, Great Ormond Street Hospital for Children NHS Trust, Great Ormond Street, London WC1N 3JH, UK  
**P Cox**, Department of Pathology, Birmingham Women's Hospital, Birmingham B15 2TG, UK  
**R C Trembath**, Division of Medical Genetics, Departments of Medicine and Genetics, University of Leicester, Leicester LE1 7RH, UK

Correspondence to: Dr C A Johnson, Section of Medical and Molecular Genetics, Department of Paediatrics and Child Health, University of Birmingham Medical School, Birmingham B15 2TT, UK; c.a.johnson@bham.ac.uk

Revised version received 1 March 2003

Accepted for publication 3 March 2003

## REFERENCES

- 1 **Jeune M**, Carron R, Beraud C, Loaec Y. Polychondrodystrophie avec blocage thoracique d'évolution fatale. *Pédiatrie* 1954;**9**:390-2.
- 2 **Oberklaid F**, Danks DM, Mayne V, Campbell P. Asphyxiating thoracic dysplasia. Clinical, radiological, and pathological information on 10 patients. *Arch Dis Child* 1977;**52**:758-65.
- 3 **Turkel SB**, Diehl EJ, Richmond JA. Necropsy findings in neonatal asphyxiating thoracic dystrophy. *J Med Genet* 1985;**22**:112-18.
- 4 **Silengo M**, Gianino P, Longo P, Battistoni G, Defilippi C. Dandy-Walker complex in a child with Jeune's asphyxiating thoracic dystrophy. *Pediatr Radiol* 2000;**30**:430.
- 5 **Kozlowski K**, Masel J. Asphyxiating thoracic dystrophy without respiratory disease. *Pediatr Radiol* 1976;**5**:30-3.
- 6 **Elejalde BR**, Mercedes de Elejalde M, Pansch D. Prenatal diagnosis of Jeune syndrome. *Am J Med Genet* 1985;**21**:433-8.
- 7 **Hudgins L**, Rosengren S, Treem W, Hyams J. Early cirrhosis in survivors with Jeune thoracic dystrophy. *J Pediatr* 1992;**120**:754-6.
- 8 **Labrunne P**, Fabre M, Trioche P, Estournet-Mathiaud B, Grangeopont MC, Rambaud C, Maurage C, Bernard O. Jeune syndrome and liver disease: report of three cases treated with ursodeoxycholic acid. *Am J Med Genet* 1999;**87**:324-8.
- 9 **Wilson DJ**, Weleber RG, Beals RK. Retinal dystrophy in Jeune's syndrome. *Arch Ophthalmol* 1987;**105**:651-7.
- 10 **Nagai T**, Nishimura G, Kato R, Hasegawa T, Ohashi H, Fukushima Y. Del(12)(p11.2;p12.2) associated with an asphyxiating thoracic dystrophy or chondroectodermal dysplasia-like syndrome. *Am J Med Genet* 1995;**55**:16-18.
- 11 **Herron BJ**, Lu W, Rao C, Liu S, Peters H, Bronson RT, Justice MJ, McDonald JD, Beier DR. Efficient generation and mapping of recessive developmental mutations using ENU mutagenesis. *Nat Genet* 2002;**30**:185-9.
- 12 **Romero R**, Pilu G, Jeanty P, Ghidini A, Hobbins JC. Asphyxiating thoracic dysplasia. In: *Prenatal diagnosis of congenital anomalies*. Norwalk, Connecticut: Appleton and Lange, 1987:342-3.
- 13 **Morgan NV**, Gissen P, Malik Sharif S, Baumber L, Sutherland J, Kelly DA, Aminu K, Bennett CP, Woods CG, Mueller RF, Trembath RC, Maher ER, Johnson CA. A novel locus for Meckel-Gruber syndrome, MKS3, maps to chromosome 8q24. *Hum Genet* 2002;**111**:456-61.
- 14 **Cottingham RW**, Idury RM, Schaffer AA. Faster sequential genetic linkage computations. *Am J Hum Genet* 1993;**53**:252-63.
- 15 **Broman KW**, Murray JC, Sheffield VC, White RL, Weber JL. Comprehensive human genetic maps: individual and sex-specific variation in recombination. *Am J Hum Genet* 1998;**63**:861-9.
- 16 **Kong A**, Gudbjartsson DF, Sainz J, Jonsson GM, Gudjonsson SA, Richardson B, Sigurdardottir S, Barnard J, Hallbeck B, Masson G, Shlien A, Palsson ST, Frigge ML, Thorgerirsson TE, Gulcher JR, Stefansson K. A high-resolution recombination map of the human genome. *Nat Genet* 2002;**31**:241-7.
- 17 **Schuermann MJ**, Otto E, Becker A, Saar K, Ruschendorf F, Polak BC, Ala-Mello S, Hoefele J, Wiedensohler A, Haller M, Omran H, Nurnberg P, Hildebrandt F. Mapping of gene loci for nephronophthisis type 4 and Senior-Loken syndrome, to chromosome 1p36. *Am J Hum Genet* 2002;**70**:1240-6.
- 18 **Casteels I**, Demandt E, legius E. Visual loss as the presenting sign of Jeune syndrome. *Eur J Pediatr Neurol* 2000;**4**:243-7.
- 19 **Hsu DR**, Economids AN, Wang X, Eimon PM, Harland RM. The Xenopus dorsalizing factor gremlin identifies a novel family of secreted proteins that antagonize BMP activities. *Mol Cell* 1998;**1**:673-83.
- 20 **Topol LZ**, Bardot B, Zhang Q, Resau J, Huillard E, Marx M, Calothy G, Blair DG. Biosynthesis, post-translation modification, and functional characterization of Dm/Gremlin. *J Biol Chem* 2000;**275**:8785-93.
- 21 **Brunet LJ**, McMahon JA, McMahon AP, Harland RM. Noggin, cartilage morphogenesis, and joint formation in the mammalian skeleton. *Science* 1998;**280**:1455-7.
- 22 **Larain J**, Bachiller D, Lu B, Agius E, Piccolo S, De Robertis EM. BMP-binding modules in chordin: a model for signalling regulation in the extracellular space. *Development* 2000;**127**:821-30.
- 23 **Brunkow ME**, Gardner JC, van Ness J, Paepfer BW, Kovacevich BR, Proll S, Skonier JE, Zhao L, Sabo PJ, Fu Y-H, Alisch RS, Gillett L, Colbert T, Tacconi P, Galas D, Hamersma H, Beighton P, Mulligan JT. Bone dysplasia sclerosteosis results from loss of the SOST gene product, a novel cystine knot-containing protein. *Am J Hum Genet* 2001;**68**:577-89.
- 24 **Zúñiga A**, Haramis A-PG, McMahon AP, Zeller R. Signal relay by BMP antagonism controls the SHH/FGF4 feedback loop in vertebrate limb buds. *Nature* 1999;**401**:598-602.
- 25 **Woychik RO**, Mass RL, Zeller R, Vogt TF, Leder P. Formins: proteins deduced from the alternative transcripts of the limb-deformity gene. *Nature* 1990;**346**:850-3.
- 26 **Mass RL**, Zeller R, Woychik RP, Vogt TF, Leder P. Disruption of formin-encoding transcripts in two mutant limb deformity alleles. *Nature* 1990;**346**:853-5.